

Supporting Information:

Thermodynamics of Sodium-Lead Alloys for Negative Electrodes from First-Principles

Damien K. J. Lee,[†] Zeyu Deng,[†] Gopalakrishnan Sai Gautam,[‡] and
Pieremanuele Canepa^{*,†,¶,§}

[†]*Department of Materials Science and Engineering, National University of Singapore, 9
Engineering Drive 1, 117575 Singapore, Singapore*

[‡]*Department of Materials Engineering, Indian Institute of Science, 560012 Bangalore,
India*

[¶]*Department of Electrical and Computer Engineering, Houston, TX 77204, USA*

[§]*Texas Center for Superconductivity, University of Houston, Houston, TX 77204, USA*

E-mail: pcanepa@uh.edu

1 Structure Characteristics of NaPb Intermetallics.

Table S1: Computed lattice parameters (in Å), space groups, and volume per atom (in $\text{\AA}^3 \cdot \text{atom}^{-1}$) of all Na-Pb intermetallics.

Formula	Space Group	<i>a</i>	<i>b</i>	<i>c</i>	V	Ref.
Pb	<i>Fm\bar{3}m</i>	5.028	—	—	31.780	S1
NaPb ₃	<i>Pm\bar{3}m</i>	4.941	—	—	30.154	S2
NaPb	<i>I4₁/acd</i>	10.661	—	18.039	32.035	S3
Na ₅ Pb ₂	<i>R\bar{3}m</i>	5.546	—	23.224	29.462	S4
Na ₉ Pb ₄	<i>P6₃/mmc</i>	5.513	—	30.009	30.378	S5
Na ₁₃ Pb ₅	<i>P6₃/mmc</i>	5.551	—	40.439	29.977	S4
Na ₁₅ Pb ₄	<i>I\bar{4}3d</i>	13.338	—	—	31.221	S6
Na	<i>Im\bar{3}m</i>	4.192	—	—	36.837	S7

Table S2: Experimental lattice parameters (in Å), space groups, and deviation from computed lattice parameters (Δ in %) of all Na-Pb intermetallics.

Formula	Space Group	<i>a</i>	<i>b</i>	<i>c</i>	Δ	Ref.
Pb	<i>Fm\bar{3}m</i>	4.950	—	—	+1.58	S1
NaPb ₃	<i>Pm\bar{3}m</i>	4.888	—	—	+1.08	S2
NaPb	<i>I4₁/acd</i>	10.580	—	17.746	+1.21	S3
Na ₅ Pb ₂	<i>R\bar{3}m</i>	5.540	—	23.150	-0.43	S4
Na ₉ Pb ₄	<i>P6₃/mmc</i>	5.470	—	30.410	-0.27	S5
Na ₁₃ Pb ₅	<i>P6₃/mmc</i>	5.510	—	40.390	+0.43	S4
Na ₁₅ Pb ₄	<i>I\bar{4}3d</i>	13.020	—	—	+2.44	S6
Na	<i>Im\bar{3}m</i>	4.300	—	—	-2.51	S7

2 Spin-orbit coupling effects

Since Pb is a heavy element, spin-orbit effects might be present in the system. Using the determined ground state structures on the convex hull, we compared the differences between our PBE calculations and the spin-orbit coupling (SOC)-included calculations (Figure S1). These SOC effects also include the zeroth-order-regular approximation that accounts for the relativistic mass correction in the SOC operator. There is an average of -15.6 meV/atom difference between the SOC and PBE calculations. This difference is well within the range of DFT formation energy errors,^{S8,S9} and the convex hull points were unaffected. Therefore,

we do not expect the inclusion of SOC effects to significantly change our results and have elected to perform the rest of our calculations without the inclusion of SOC effects.

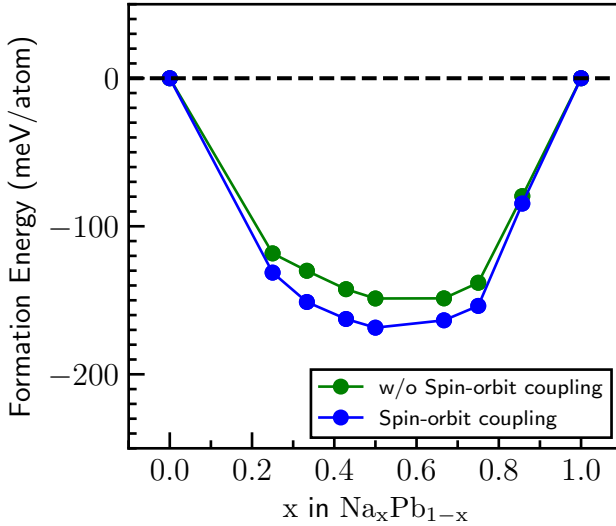


Figure S1: Formation energies of the ground state FCC orderings for the PBE calculations (green) and the PBE-SOC calculations (blue). The average difference between the formation energies obtained with the PBE-SOC and PBE calculations is -15.6 meV/atom.

3 Cluster Expansion Coefficients

The 33 fitted effective cluster interactions (ECIs) are displayed in Table S3 and plotted in Figure S3. A negative ECI indicates energetically favorable interactions between Na and Pb for clusters while a positive ECI indicates unfavourable interactions between atoms of similar species.

Table S3: Effective cluster interactions (ECIs in meV) values of the Point, Pair, Triplet, and Quadraplet terms. Cell [0, 0, 0] is the reference cell. M refers to the multiplicity of each cluster. Maximum (Max.) and Minimum (Min.) cluster lengths are in Å.

Index	Cluster Index	Cluster type	Cell	M	Min.	Max.	ECI	ECI/M
0	0	Empty	—	1	0.000	0.000	-113.436	-113.436
1	1	Point	[0, 0, 0]	1	0.000	0.000	-14.220	-14.220
2	2	Pair	[0, 0, 0][0, 1, 0]	6	3.500	3.500	119.944	19.991
3	3	Pair	[0, 0, 0][1, -1, -1]	3	4.950	4.950	-1.687	-0.562
4	4	Pair	[0, 0, 0][1, -2, 1]	12	6.062	6.062	-11.092	-0.924
5	5	Pair	[0, 0, 0][0, 2, 0]	6	7.000	7.000	6.452	1.075
6	6	Pair	[0, 0, 0][3, -1, -1]	4	8.574	8.574	1.773	0.443
7	7	Pair	[0, 0, 0][0, 3, 0]	6	10.501	10.501	-2.864	-0.477
8	8	Triplet	[0, 0, 0][0, 0, 1][0, 1, 0]	8	3.500	3.500	9.574	1.197
9	9	Triplet	[0, 0, 0][0, 0, 1][1, -1, 1]	12	3.500	4.950	10.437	0.870
10	10	Triplet	[0, 0, 0][0, 0, 1][1, 0, 1]	24	3.500	6.062	-12.251	-0.510
11	11	Triplet	[0, 0, 0][0, 1, 0][1, -1, 1]	24	3.500	6.062	-18.552	-0.773
12	12	Triplet	[0, 0, 0][0, 1, 1][1, 1, 0]	24	3.500	6.062	4.501	0.188
13	13	Triplet	[0, 0, 0][0, 1, -2][0, 2, -1]	8	6.062	6.062	-2.336	-0.292
14	14	Triplet	[0, 0, 0][0, 0, 1][0, 2, -1]	48	3.500	7.000	24.069	0.501
15	15	Triplet	[0, 0, 0][0, 1, 1][2, 0, 0]	12	6.062	7.000	-6.514	-0.543
16	16	Triplet	[0, 0, 0][0, 0, 2][0, 2, 0]	8	7.000	7.000	-1.651	-0.206
17	17	Triplet	[0, 0, 0][0, 1, -2][1, -1, -2]	48	6.062	7.827	5.966	0.124
18	18	Triplet	[0, 0, 0][0, 1, -1][2, 0, 0]	24	3.500	7.827	7.520	0.313
19	19	Triplet	[0, 0, 0][1, -2, 2][2, -2, 1]	24	3.500	7.827	-3.592	-0.150
20	20	Quadruplet	[0, 0, 0][0, 0, 1][0, 1, 0][1, 0, 0]	2	3.500	3.500	1.178	0.589
21	21	Quadruplet	[0, 0, 0][0, 1, -1][0, 1, 0][1, 0, 0]	12	3.500	4.950	6.423	0.535
22	22	Quadruplet	[0, 0, 0][0, 0, 1][1, 0, 0][1, 0, 1]	12	3.500	6.062	6.600	0.550
23	23	Quadruplet	[0, 0, 0][0, 0, 1][0, 1, -1][1, -1, 0]	24	3.500	6.062	4.028	0.168
24	24	Quadruplet	[0, 0, 0][0, 1, 0][1, -1, 1][1, 0, 1]	6	3.500	6.062	2.417	0.403
25	25	Quadruplet	[0, 0, 0][0, 1, -2][0, 1, -1][0, 2, -1]	8	3.500	6.062	-3.835	-0.479
26	26	Quadruplet	[0, 0, 0][0, 1, -1][0, 1, 0][2, 0, -1]	8	3.500	6.062	3.397	0.425
27	27	Quadruplet	[0, 0, 0][0, 1, 0][1, 1, -2][2, 0, -1]	12	3.500	6.062	-4.748	-0.396
28	28	Quadruplet	[0, 0, 0][0, 0, 1][0, 2, -1][1, 1, -1]	24	3.500	7.000	-4.435	-0.185
29	29	Quadruplet	[0, 0, 0][0, 0, 1][0, 1, -1][2, 0, -1]	48	3.500	7.000	6.889	0.144
30	30	Quadruplet	[0, 0, 0][1, -1, 1][1, 1, -1][2, 0, 0]	3	4.950	7.000	2.593	0.864
31	31	Quadruplet	[0, 0, 0][1, -2, 1][1, 0, -1][2, -2, 0]	12	3.500	7.000	-3.203	-0.267
32	32	Quadruplet	[0, 0, 0][0, 0, 2][0, 2, 0][2, 0, 0]	2	7.000	7.000	-0.720	-0.360

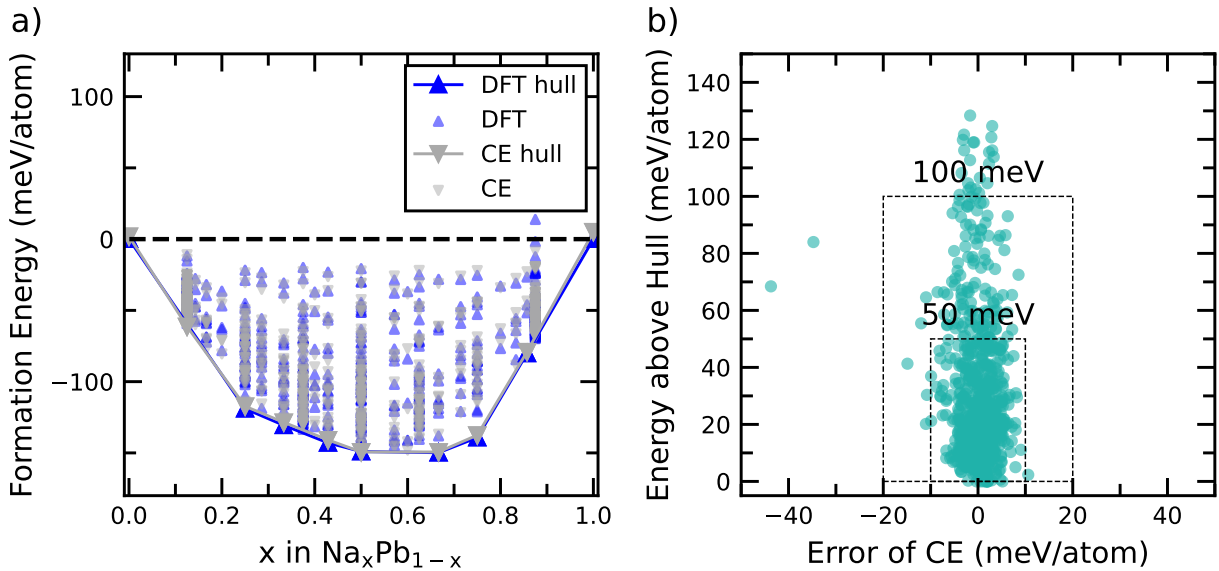


Figure S2: **a)** Formation energies of the FCC orderings (blue) and the formation energies predicted by the cluster expansion model (grey). The references used are the FCC crystal structure for pure Na and Pb. **b)** Error of the CE model with respect to DFT. The dashed lines are the confidence windows ($\pm 10 \text{ meV}\cdot\text{atom}^{-1}$ and $\pm 20 \text{ meV}\cdot\text{atom}^{-1}$ for the CE model).

4 Thermodynamic Integration

The grand canonical potential energy (Φ) is defined in Eq. 4:

$$\Phi = E - TS - \mu x \quad (1)$$

where E is the total energy predicted by the CE model, S is the configurational entropy, and μ is the parametric chemical potential set in GCMC scans. From GCMC scans at fixed μ and variable T , Φ is calculated using the thermodynamic integration of Eq. 2.

$$\beta\Phi(T, \mu) = \beta_0\Phi(T_0, \mu) + \int_{\beta_0}^{\beta} [E - \mu x] d\beta \quad (2)$$

where β is the reciprocal temperature, $1/k_B T$, k_B is the Boltzmann constant, and $\beta_0 = 1/k_B T_0$. T_0 is the reference temperature and is chosen to be 5K, in which entropic effects are negligible and hence $\Phi(T_0, \mu) = E - \mu x$. For GCMC scans at fixed T and variable μ , Φ

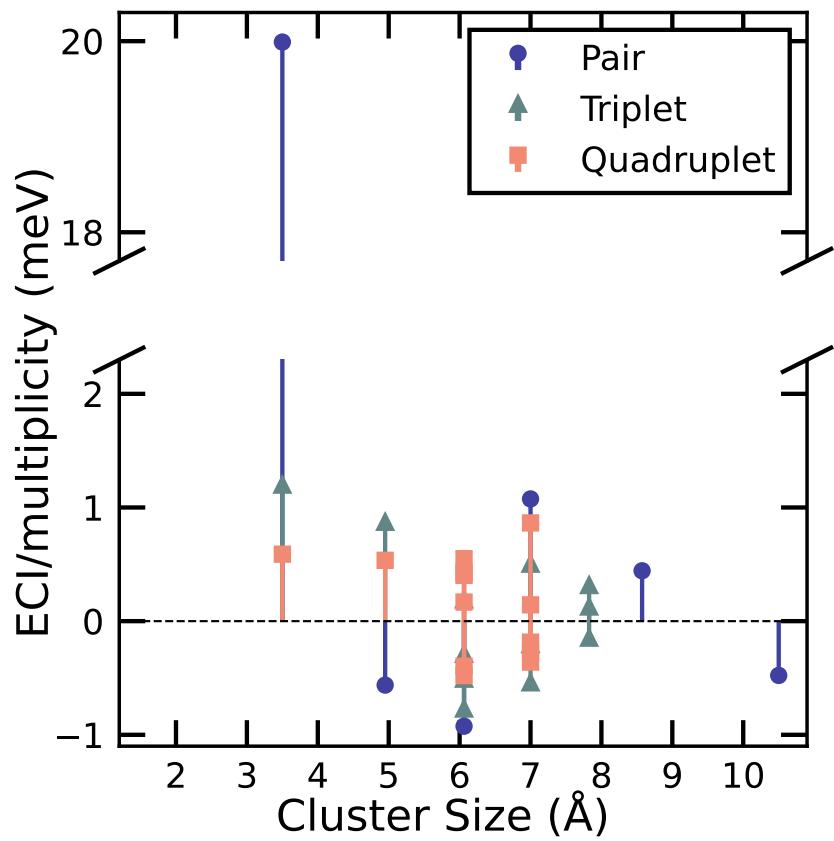


Figure S3: 33 effective cluster interactions in meV/multiplicity vs. their length (in \AA , x -axis). Negative (positive) ECIs in pairs are favourable (unfavourable) interactions between Na-Pb (Na-Na, Pb-Pb).

is calculated using thermodynamic integration in Eq. 3:

$$\Phi(T, \mu) = \phi(T, \mu_0) - \int_{\mu_0}^{\mu} x \, d\mu \quad (3)$$

Thermodynamic integration was carried out numerically with the composite trapezoidal rule.

For ordered intermetallic phases, the grand-canonical free energy can be obtained directly from Eq. 4.

$$\Phi = E - \mu x \quad (4)$$

since the configurational entropy (S) of an ordered phase is 0.

The grand canonical energies for each phase can be plotted on a single plot to determine the phase boundaries. The phase boundaries are identified from the intersections of Φ for each phase in the μ space and from the discontinuities in x vs. μ plots.

References

- (S1) Bouad, N.; Chapon, L.; Marin-Ayral, R. M.; Bouree-Vigneron, F.; Tedenac, J. C. Neutron powder diffraction study of strain and crystallite size in mechanically alloyed PbTe. *J. Solid State Chem.* **2003**, *173*, 189–195.
- (S2) Havinga, E. E.; Damsma, H.; Van Maaren, M. H. Oscillatory dependence of superconductive critical temperature on number of valency electrons in Cu₃Au-type alloys. *J. Phys. Chem. Solids* **1970**, *31*, 2653–2662.
- (S3) Marsh, R. E.; Shoemaker, D. P. The crystal structure of NaPb. **1953**, *6*, 197–205.
- (S4) Weston, N.; Shoemaker, D.; Kuhi, L.; Tse, R. The crystal structures of three phases in the Pb-Na system. **1957**, *10*, 775–775.
- (S5) Ward, L.; Michel, K.; Wolverton, C. Three new crystal structures in the Na-Pb system:

- solving structures without additional experimental input. *Acta Crystallogr. A Found. Adv.* **2015**, *71*, 542–548.
- (S6) Lamprecht, G. J.; Dicks, L.; Crowther, P. Solubility of metals in liquid sodium. II. The system sodium-lead. **1968**, *72*, 1439–1441.
- (S7) Hull., A. W. A New Method of X-Ray Crystal Analysis. *Phys. Rev.* **1917**, *10*, 661–696.
- (S8) Sun, W.; Dacek, S. T.; Ong, S. P.; Hautier, G.; Jain, A.; Richards, W. D.; Gamst, A. C.; Persson, K. A.; Ceder, G. The thermodynamic scale of inorganic crystalline metastability. *Sci. Adv.* **2016**, *2*, e1600225.
- (S9) Wang, A.; Kingsbury, R.; McDermott, M.; Horton, M.; Jain, A.; Ong, S. P.; Dwaraknath, S.; Persson, K. A. A framework for quantifying uncertainty in DFT energy corrections. *Sci. Rep.* **2021**, *11*, 15496.